Effect of Block Length on Solvent Response of Block Copolymer Brushes: Combinatorial Study with Block Copolymer Brush Gradients

Chang Xu,[†,‡] Tao Wu,[†] Charles Michael Drain,[‡] James D. Batteas,[†,§] Michael J. Fasolka,[†] and Kathryn L. Beers*[,†]

Polymers Division and Surface and Microanalysis Science Division, National Institute of Standards and Technology, 100 Bureau Drive, Gaithersburg, Maryland 20899, and Department of Chemistry and Biochemistry, Hunter College and the Graduate Center of The City University of New York, 695 Park Avenue, New York, New York 10021

Received June 29, 2005; Revised Manuscript Received February 2, 2006

ABSTRACT: Block copolymer (BC) brush gradient libraries were examined as high-throughput platforms to study the effect of relative block lengths on the response to solvents. BC brushes of poly(*n*-butyl methacrylate) (PBMA) and poly(2-(*N*,*N*′-dimethylamino)ethyl methacrylate) (PDMAEMA) were synthesized via surface-initiated atom transfer radical polymerization (ATRP). The gradient libraries had uniform bottom PBMA blocks and molecular mass gradient top PDMAEMA blocks. The rearrangement of the BC brushes upon exposure to water and hexane was assessed by water contact angle (θ_w) measurements. θ_w mapping of each gradient library illustrated how the top PDMAEMA block length influenced the response of BC brushes to solvents. Comparison among libraries with different bottom PBMA thicknesses revealed how the bottom block length affected the solvent response of BC brushes. Our results indicate that the solvent response behavior of the BC brushes is greatly influenced by their relative block lengths. While surface response properties can be suppressed by a long top block, they can be enhanced by the extension of the bottom block. In addition, our work suggests that BC brushes could be fabricated to provide tunable surfaces with gradient responsive properties.

Introduction

Surface properties of materials are essential to their interactions with environments. The advancement of new technologies, such as micro- and nano-electromechanical systems, novel sensors, and new biomaterials, demands precise control of surface properties such as adhesion, friction, environmental response, and biocompatibility.[1−3] Grafting surfaces with polymer brushes provides a versatile way to modify surface properties.[4,5] For example, tethered block copolymers (BCs) or mixtures of polymers have been used to create surfaces with responsive properties.[6−14] Selectively treating these surfaces with solvents favoring one component/segment of the polymer exposed that specific component/segment to the surface, resulting in changes of surface properties.

Previous theoretical and experimental results demonstrate that various factors, such as grafting density, molecular weight, chemical composition, solvents, and temperature, may affect the properties of polymer brushes.[15−24] To rapidly and thoroughly examine the effect of these variables on brush behavior, a variety of combinatorial methods have been developed during recent years. For example, Genzer et al. exploited a grafting density gradient to investigate how the grafting density affects swelling behavior of polymer brushes.[15,16] With specimens that had relative grafting density gradients of two distinct polymer brushes, Stamm et al. and Zhao et al. studied the effect of relative density on the solvent-induced rearrangement of mixed brushes.[25,26]

In the above cases, gradient substrates with systematic variations across the surface were synthesized and utilized as high-throughput platforms to study how those variables affect the properties of polymer brushes. Several methods have been developed to synthesize polymer brush-modified substrates with gradient properties such as grafting density, molecular mass, and chemical composition.[15,27−29] Moreover, based on a polymer brush molecular mass gradient, a synthetic approach for the preparation of BC brush gradients was demostrated.[30,31]

Recent development of surface-initiated polymerization[4,5] provides a facile way to synthesize grafted polymer brushes with control of gradient profiles. In this approach, initiating functionality is first immobilized on the surface. Subsequent polymerization from the surface-immobilized initiator moieties leads to the formation of tethered polymers on surfaces. Among various types of polymerization methods,[32−39] surface-initiated atom transfer radical polymerization (ATRP)[32−34] has attracted much attention for its controlled/living character, tolerance of functional groups, and mild experimental requirements. A variety of homo- and copolymer brushes have been synthesized with ATRP.[9−16,27−34,41]

In this work, we demonstrate a combinatorial method to study the influence of relative block length on the solvent responsive behavior of BC brushes. To achieve this goal, a BC brush gradient was designed and synthesized via surface-initiated ATRP. Unlike the copolymer brush gradient synthesized by Genzer et al., which has a gradient bottom block, the polymer brush gradient synthesized in this work had a uniform poly(*n*-butyl methacrylate) (PBMA) bottom block and a molecular mass gradient poly(2-(*N*,*N*′-dimethylamino)ethyl methacrylate) (PDMAEMA) top block. With PDMAEMA gradient samples that have different PBMA layer thicknesses, copolymer brush libraries with controlled variations of individual block length were established. The gradient libraries were employed to map the solvent response behavior of BC brushes, which was evaluated by surface water contact angle (θ_w) measurement.

[†] National Institute of Standards and Technology.
[‡] Hunter College and the Graduate Center of The City University of New York.
[§] Current address: Department of Chemistry, Texas A&M University, College Station, TX 77842.
* Corresponding author. E-mail: Kathryn.Beers@nist.gov.

10.1021/ma051405c CCC: $33.50
Published on Web 03/31/2006

Experimental Section[41]

Materials. 2-(*N*,*N*′-Dimethylamino)ethyl methacrylate (DMAEMA) (99%) was purchased from Polysciences. Copper(I) bromide (CuBr, 99%, Aldrich) was purified by stirring in acetic acid, washing with methanol, and drying under vacuum. Copper(II) bromide ($CuBr_2$, 99%), 2,2′-bipyridyl (bpy, 99+%), *n*-butyl methacrylate (BMA; 99%), methylene chloride (99.9%, HPLC grade), hexane (98.5% ACS grade), *N*,*N*′-dimethylformamide (DMF, 99.8%, HPLC grade), acetone (99.5%, ACS grade), and anhydrous toluene (99.8%) were purchased from Aldrich. 2-Propanol (HPLC grade) was ordered from J.T. Baker. Water was purified through a Millipore Rios 16 system. Single-side-polished silicon (100) wafers were purchased from Wafer World Inc., and double-side-polished silicon (100) wafers were purchased from Silicon Inc. A BS-8000 programmable syringe pump (Braintree Scientific, Inc.) was used to control the infusion rate of the reaction mixture into the polymerization flask.

Initiator-Modified Silicon Substrate. Preparation and modification of the silicon surface with initiator self-assembled monolayers (SAMs) were reported in a previous work.[29] Briefly, the initiator, 11-(2-bromo-2-methyl)propionyloxy-undecyltrichlorosilane, was synthesized according to the literature procedure[33] and diluted with anhydrous toluene to a concentration of 0.5 mmol/L. Silicon wafer sections (1.6 cm × 3 cm for uniform sample, 1.2 cm × 8 cm for gradient sample) were rinsed with acetone and ultraviolet ozone cleaned for 30 min. The wafer was immersed into the initiator solution overnight to ensure the complete formation of initiator SAMs on the surface. Following toluene and acetone rinses, the substrate was dried under a flow of nitrogen. The thickness of the initiator SAMs is 2 ± 0.2 nm according to ellispsometry measurement. For polymer brushes prepared for IR analysis, double-side-polished silicon wafers were used to prevent light from scattering at the rough surface. In all other cases, single-side-polished silicon wafers were used.

Preparation of Polymerization Solutions. CuBr (19.2 mg, 13.4 mmol), $CuBr_2$ (3.3 mg, 1.5 mmol), bpy (49.2 mg, 32 mmol), and a stirring bar were added to a flask and capped with a rubber septum. After three cycles of vacuum and backfilling with argon, 4.5 mL of degassed 2-propanol, 0.5 mL of degassed H_2O, and 5 mL of degassed monomer (BMA or DMAEMA) were sequentially syringed into the flask. The polymerization mixture was stirred for 1 h.

Synthesis of Surfaces with Uniform Polymer Brushes. An initiator-modified silicon substrate was placed in a flask and sealed with a rubber septum. Following three cycles of vacuum and backfilling with argon, the flask was quickly filled with the above prepared polymerization mixture by syringe, and the whole substrate was immersed in the polymerization solution. After a certain period of polymerization at room temperature, the substrate was taken from the reaction mixture, thoroughly rinsed with DMF, and dried under a flow of nitrogen. To synthesize BC brushes with a uniform top block, the same procedures described above were applied to a polymer-brush-modified substrate.

Synthesis of Polymer Brush Gradients. An initiator/polymer-modified silicon substrate (1.2 cm × 8 cm) was placed upright in a 1.4 cm diameter test tube, sealed with a rubber septum, and deoxygenated by three cycles of vacuum and argon backfill. The polymerization solution was transferred into a 10 mL syringe, which then was mounted on a syringe pump. The polymerization solution was slowly pumped into the test tube along its sidewall at a rate of 100 μL/min. After a given period of time, the pumping process ceased. The substrate was removed from the tube, rinsed with DMF, and dried under a flow of nitrogen.

Solvent Treatment of the Surface. Hexane and water were used to treat the brush-modified surfaces. To facilitate the segment rearrangement, methylene chloride, acetone, and methanol were used as intermediate solvents. For example, to check the surface properties after water treatment, the sample was sequentially immersed in methylene chloride, acetone, and methanol before exposure to water. For hexane treatment, the reverse sequence was applied. For each solvent treatment, the substrate was immersed in the solvent for 30 min and then dried under a flow of nitrogen.

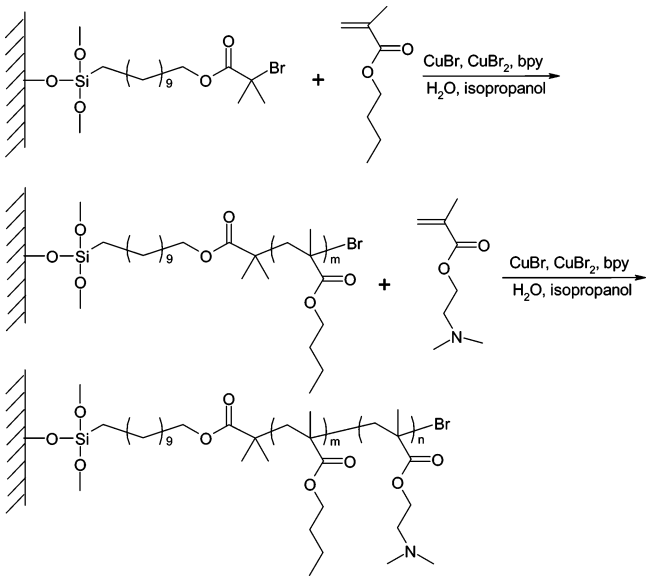

Figure 1. Synthesis of copolymer brushes of poly(*n*-butyl methacrylate) and poly(2-(*N*,*N*′-dimethylamino)ethyl methacrylate) via surface-initiated atom transfer radical polymerization.

Measurement Methods. Spectroscopic ellipsometry (VASE, J.A. Woollam Co., Inc.) was used to measure the thickness of the SAMs and polymer brushes. Static water contact angle (θ_w) was measured using a Krüss G2 contact angle goniometer. The standard uncertainties for the ellipsometry and θ_w measurement are 0.5 nm and 3°, respectively. Transmission FT-IR spectra were measured on a Nicolet Magna-IR 860 spectrometer at the Brewster's angle for silicon (74°). Each spectrum was collected with 512 scans at an 8 cm^{-1} resolution.

Results and Discussion

Surface-Initiated Atom Transfer Radical Polymerization (ATRP) of BMA and DMAEMA. Figure 1 outlines the surface-initiated ATRP of BMA and DMAEMA. The polymerization conditions used in this work are similar to the solution ATRP of BMA and DMAEMA reported by Matyjaszewski et al.[42] However, in our experiment, the free initiator in solution was replaced by initiator-modified substrates. Because of the extremely small amount of initiator moieties present in the polymerization, we did not assume that the surface-initiated polymerization was also controlled. Accordingly, the kinetics of surface-initiated polymerization of BMA and DMAEMA were first characterized.

Recently, it was demonstrated that the kinetics of surface-initiated polymerization could be combinatorially studied by varying the polymerization time at different locations on the substrate.[27] A similar approach was adopted in this study. During the polymerization, solutions were gradually pumped into the reaction flask at a controlled rate. As the solution level increased, the substrate was gradually immersed. After a certain period of time, the whole substrate was removed from the polymerization solution. Areas located at the bottom of the flask had longer polymerization time than those at the top. Figure 2 shows the results of such polymerization of BMA and DMAEMA. For both monomers, we observed linear growth of polymer brush thickness with polymerization time. We assume, therefore, that all active chain ends propagate simultaneously, and the dry polymer brush thickness is directly proportional to its number-average molecular mass. These results suggested that the

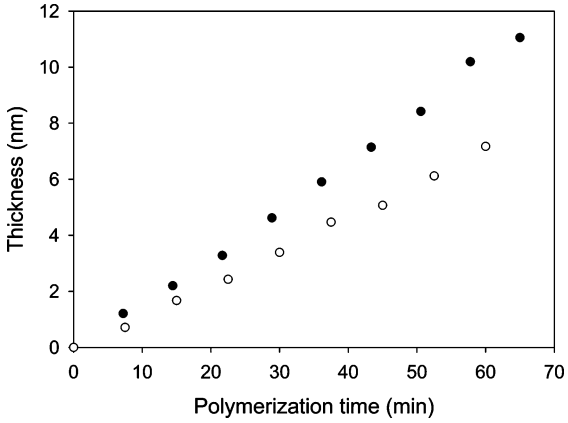

Figure 2. Kinetics of homopolymer brush growth of (●) poly(*n*-butyl methacrylate) (PBMA) and (○) poly(2-(*N*,*N*′-dimethylamino)ethyl methacrylate) (PDMAEMA). Polymerization conditions: [CuBr] = 13.4 mmol, [$CuBr_2$] = 1.5 mmol, [bipyridine] = 32 mmol, monomer (BMA or DMAEMA):2-propanol:H_2O = 50:45:5 (v:v:v).

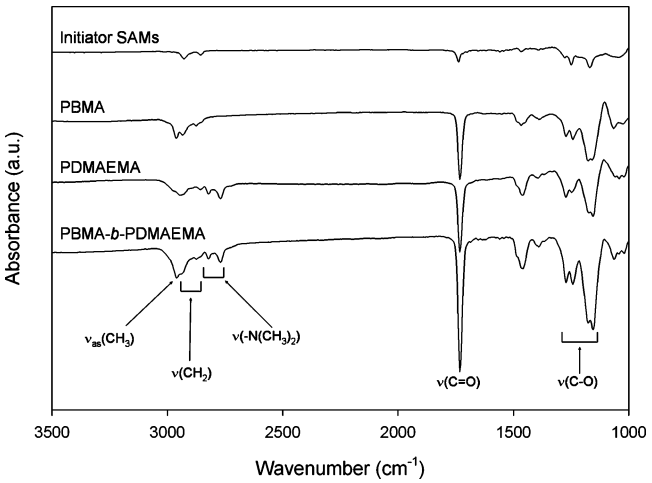

Figure 3. FT-IR of (co)polymer brushes synthesized from surface-initiated polymerization: (1) initiator self-assembled monolayers (SAMs), (2) poly(*n*-butyl methacrylate) (PBMA), (3) poly(2-(*N*,*N*′-dimethylamino)ethyl methacrylate) (PDMAEMA), and (4) PBMA-*b*-PDMAEMA.

polymerization processes were controlled under current conditions, and the thickness or molecular mass of the polymer brushes could be readily controlled with polymerization time.

Block Copolymer Brush Synthesis. Prior to the synthesis of BC brush gradients, we synthesized uniform BC brushes of PBMA and PDMAEMA. The chemistries of the resulting polymer brushes were characterized by transmission FT-IR.

To synthesize BC brushes, the initiator-modified substrate was first polymerized in BMA solution for 40 min, and the film thickness increased by 6.5 nm. Subsequent polymerization of DMAEMA for 1 h added 7.6 nm to the total film thickness. Under the same conditions, 7.5 nm thick PDMAEMA homopolymer brushes were synthesized from the initiator-modified substrate.

IR spectra for substrates with initiator monolayers only, PBMA, PDMAEMA, and PBMA-*b*-PDMAEMA brushes are shown in Figure 3. The characteristic peak for the C═O group was at 1736 cm^{-1}. Peaks at 1254 and 1159 cm^{-1} were attributed to C−O stretching. The peaks at 2854 and 2927 cm^{-1} were assigned to the C−H symmetric and asymmetric vibration modes, respectively, of the $-CH_2-$ groups. The existence of C═O, CH_2, and C−O peaks in the sample with initiator only confirmed that initiator was immobilized on the Si wafer

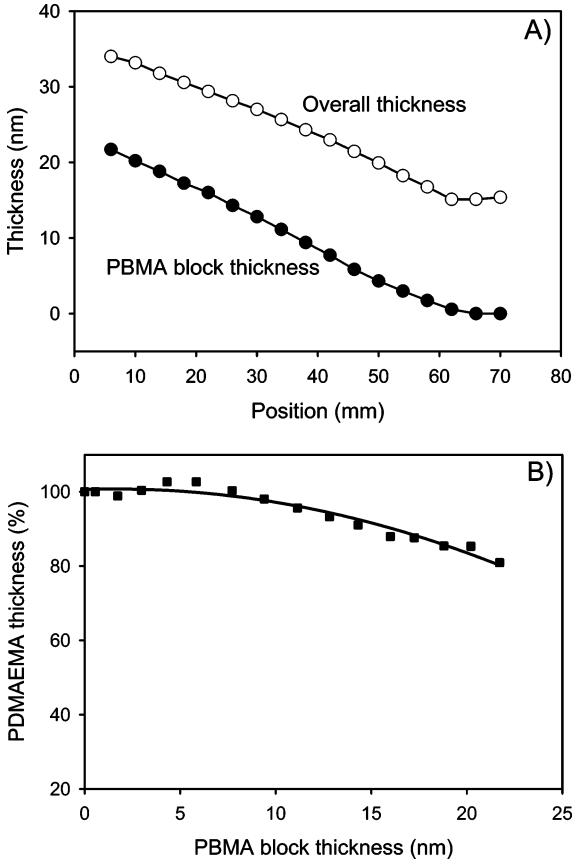

Figure 4. Effect of the poly(*n*-butyl methacrylate) (PBMA) block length on the growth of the second poly(2-(*N*,*N*′-dimethylamino)ethyl methacrylate) (PDMAEMA) block. (A) Polymer brush thickness after polymerization of PBMA (●) and subsequent polymerization of PDMAEMA (○). (B) Percentage growth of PDMAEMA block on the gradient surface with respect to a bare initiator-modified surface. Line in (B) is added to guide the eye.

surfaces. After the polymerization of either BMA or DMAEMA, the intensity of these characteristic peaks increased along with increased film thickness, indicating the growth of methacrylate-based polymers on the surface. The *n*-butyl group of the PBMA brush contributed to the much higher intensity of the peak at 2980 cm^{-1}. The spectrum of the PDMAEMA sample clearly showed two extra peaks at 2819 and 2769 cm^{-1}, which were attributed to C−H vibrations of $-N(CH_3)_2$. The IR spectrum of the PBMA-*b*-PDMAEMA brush contained all characteristic peaks of both homopolymer brushes. Furthermore, its peak intensities are consistent with the overall intensities of the corresponding peaks in the spectra of the two homopolymer brushes. Thus, in addition to the ellipsometry results, IR spectra further confirmed the successful synthesis of a BC brush.

Effects of PBMA Layer Thickness on Initiation of DMAEMA. Before preparing gradient copolymer brushes, we assessed how the PBMA layer thickness affects the growth of the PDMAEMA block. For this purpose, we prepared a molecular mass gradient PBMA substrate with a thickness range of 0 nm at one end to 23 nm at the other. The substrate was fully immersed into a polymerization solution of DMAEMA. After 2 h of polymerization, the substrate was removed from the polymerization solution. As shown in Figure 4a, polymer brush thickness increased over the entire surface. The bare initiator-modified surface provided an internal standard to calibrate the influence of the PBMA brush layer thickness on initiation efficiency for the PDMAEMA block. Figure 4b shows the thickness of the second PDMAEMA block on the gradient

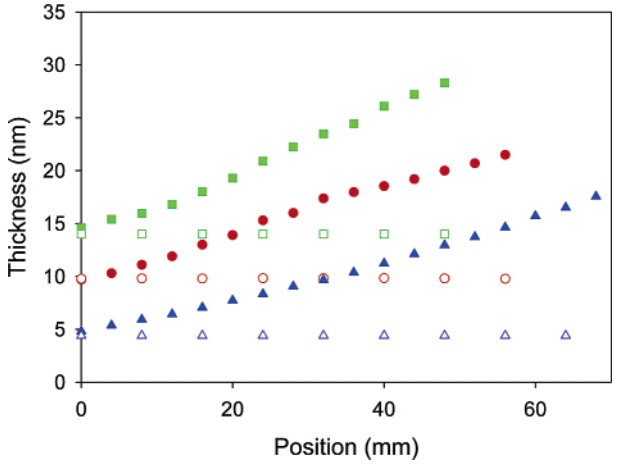

Figure 5. Thickness profiles of the block copolymer gradients synthesized. Open symbols: thickness of the substrate after polymerization of *n*-butyl methacrylate (BMA). Filled symbols: the overall thickness of the gradient after polymerization of 2-(*N*,*N*′-dimethylamino)ethyl methacrylate (DMAEMA). (blue symbols, ▲, △) Gradient I, (red symbols, ●, ○) gradient II, and (green symbols, ■, □) gradient III.

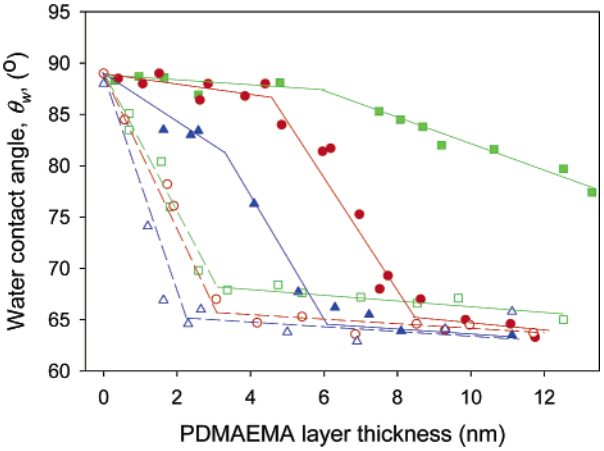

Figure 6. Surface water contact angle after hexane (filled symbols) and water (open symbols) treatment of copolymer brush gradient surfaces: (blue symbols, ▲, △) gradient I, (red symbols, ●, ○) gradient II, and (green symbols, ■, □) gradient III. Lines are added to guide the eye.

PBMA substrate as a percentage of that measured on bare initiator SAMs. Generally, the growth of the second block decreased with increasing PBMA thickness. We attribute this to a decrease in PBMA chains reinitiating to add a PDMAEMA segment. However, relatively high initiation efficiency (compared to initiation from a simple SAM-functionalized surface) was maintained across the gradient. For PBMA blocks up to 15 nm thick, subsequent growth, and presumably the grafting density, of PDMAEMA was at least 90% of that of initiator SAMs. Below this point, the small change in initiating efficiency enabled independent study of the bottom PBMA block length effect on BC brush properties.

Block Copolymer Brush Gradient Synthesis. Figure 5 summarizes the thickness profiles of the BC brush gradients prepared for this study. The BC brush gradients were synthesized in two steps. First, homogeneous polymerization of BMA results in a PBMA brush of uniform thickness across the substrate, which was predetermined by the polymerization time. Three substrates with PBMA brush thicknesses of 4.4, 9.7,[31] and 14.1 nm were synthesized. Second, with the same technique used to synthesize the homopolymer brush gradient, subsequent polymerization of DMAEMA from the homogeneous PBMA brushes resulted in BC brush gradients. The slope of the gradient was controlled by the pumping rate of the polymerization solution into the reaction flask. All three substrates reflect a linear increase of the top PDMAEMA layer thickness from 0 nm at one end to more than 12 nm at the other end of the substrate.

Solvent Response of BC Brushes. The BC brush gradient libraries provided a high throughput pathway to elucidate how relative layer thickness or block length affects the properties of BC brushes. Hexane and water were chosen to treat the gradient surfaces. While water is a better solvent for PDMAEMA, hexane is a better solvent for PBMA.

The water contact angle, θ_w, mapping of the gradient surfaces after solvent treatment is shown in Figure 6. Homopolymer brushes of PBMA and PDMAEMA exhibited contact angles of 89° and 65°, respectively. In the following discussion, these values are taken as benchmarks indicating either a PBMA or PDMAEMA homopolymer surface.

The response of the system to water treatment is discussed first. In this case, the effect of the length of the PDMAEMA is evident in the surface chemistry of the system as measured by θ_w. For all three gradient substrates, with increasing PDMAEMA thickness (h_{PD}), θ_w decreased until it became close to the characteristic value of PDMAEMA. Despite slight variation among the three substrates, a thin PDMAEMA top block ($h_{PD} > 2-3$ nm) resulted in an observed θ_w value close to that of PDMAEMA homopolymer brushes. Further increase in h_{PD} did not affect θ_w.

As shown in Figure 6, the surface response to hexane treatment varied greatly over the three gradients examined. For the block copolymer with a 4.4 nm PBMA block (gradient I), changes in surface properties are immediately evident upon introduction of a PDMAEMA block, where θ_w decreased with increase of h_{PD}. This trend continued until h_{PD} reached 6 nm, where θ_w is characteristic of PDMAEMA. Beyond this point, θ_w stabilized at that for PDMAEMA, and the surface exhibited the same wetting behavior after both hexane and water treatment.

For the substrate with a 9.7 nm PBMA block (gradient II), the presence of a thin PDMAEMA layer on the PBMA block had little effect on the θ_w of the surface after hexane treatment, which is close to that of PBMA homopolymer brushes. However, after h_{PD} reached ≈5 nm, there was a sharp decrease of θ_w with the increase of h_{PD}. This decrease of θ_w continued until h_{PD} reached ≈9 nm, where the characteristic θ_w value of PDMAEMA was measured.

For the substrate with a 14.1 nm PBMA block (gradient III), after hexane treatment the θ_w resembled that of PBMA homopolymer in regions where the h_{PD} was less than 7 nm. Above this thickness, θ_w gradually decreased with increasing of h_{PD}. The slope of the θ_w change was much smaller than that of the previous two gradients. Even for the surface areas with the largest h_{PD} studied (≈13.5 nm), the θ_w never reached the value characteristic of PDMAEMA.

The wetting properties of surfaces depend on both chemical composition and roughness.[43,44] For block copolymer brushes, the collapse of the top block into the bottom block has been reported to lead to a change of surface topography.[10] Atomic force microcopy (AFM) was used to map the surface topography of gradient II after treatment with each solvent (images in Supporting Information). After water treatment, the surface was relatively smooth with a root-mean-square (rms) roughness of approximately 0.7−1 nm. After hexane treatment, the surface topography changed depending on the PDMAEMA block thickness. For short PDMAEMA blocks ($h_{PD} < 4$ nm), the

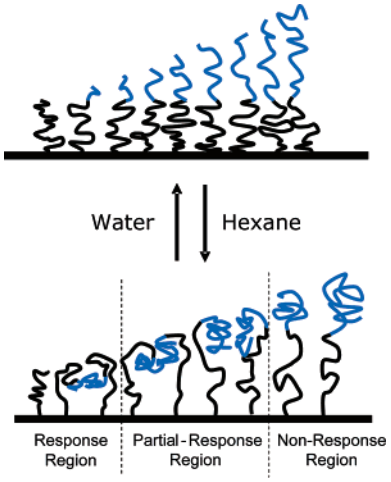

Figure 7. Schematic illustration of three regions of the block copolymer brushes after hexane treatment. Black segments represent poly(*n*-butyl methacrylate). Blue segments represent poly(2-(*N*,*N*′-dimethylamino)-ethyl methacrylate).

surface exhibited a dimpled morphology. The lateral size and spacing of these undulations increased with increasing PDMAEMA block thickness. However, for the longer PDMAEMA blocks ($h_{PD} > 4$ nm) the surface was relatively smoother. Across the whole substrate, the rms roughness of the surface was less than 1.5 nm. Therefore, we propose that variations of surface contact angle mainly reflect surface composition changes; for example, an increase in θ_w indicates an increase of PBMA segments on the surface.

As illustrated schematically in Figure 7, our measurements suggest that water treatment of the surface brings the PDMAEMA block to the surface. When the PDMAEMA segment is more than 3 nm thick, the surface properties are dominated by PDMAEMA. Below this critical thickness, the PDMAEMA segments could not effectively shield PBMA from the surface, resulting in a θ_w higher than that expected from complete surface coverage by PDMAEMA.

After hexane treatment, the PBMA segments tend to segregate to the surface while the PDMAEMA block collapses. If the PDMAEMA block is short enough, the structure can be easily covered by the PBMA block, and the surface properties resemble that of PBMA. This results in a "response region", wherein surface composition is driven by solvent treatment. In the region, windows of maximum possible surface property were exhibited by gradients II and III; here, solvent treatment drives complete surface composition switches from PBMA to PDMAEMA. As the PDMAEMA block length increases, it becomes more difficult for the bottom PBMA block to cover the surface. Our θ_w measurements suggest that in this "partial-response region" hexane treatment results in a mixture of PBMA and PDMAEMA segments at the surface, with increasing PDMAEMA content as the PDMAEMA block length is increased. The partial response region ends where the PBMA segment can no longer be expressed at the surface under hexane treatment. Beyond this point, there exists a "non-response region", where the surface is dominated by PDMAEMA regardless of solvent treatment.

This behavior can be understood by considering the barriers to segment rearrangement. If they are to be expressed at the surface of the brush, the surface-anchored PBMA segments must stretch to overcome the barrier exhibited by the top PDMAEMA block. This stretching barrier does not exist for the top PDMAEMA block, but collapsed PDMAEMA blocks have to be accommodated by rearrangement of the PBMA segments. For both of these reasons, the response region and partial-response region become wider as the PBMA block length increases. For similar reasons, the response range (extent of surface expression switch) also increases in the response and partial response regions as the PBMA block is lengthened.

Responsive Gradient Surface. Our results also indicate that BC brush gradients could be used to construct responsive gradient surfaces, which exhibit gradient surface characteristics that could be turned "on" or "off" by environmental stimuli. This type of response is observed in the partial-response region of gradient II. After hexane treatment, for h_{PD} between 5 and 9 nm, the θ_w of the surface decreases along the substrate. Within the same region, we observed a constant θ_w after water treatment. Similar behavior was noted in gradient III, but over a broader range of thickness. In this case, the transition started from $h_{PD} \approx 7$ nm and did not end, even at $h_{PD} \approx 13.5$ nm. This indicates that the switchable surface gradient can be tuned by the thickness of the bottom PBMA block and the span of the top PDMAEMA thickness gradient.

Conclusion

In summary, we used BC brush gradients to systematically study the influence of individual block length on the solvent response behavior of PBMA-*b*-PDMAEMA brushes. The synthesized gradients had a uniform bottom PBMA block and a molecular mass gradient top PDMAEMA block. After water treatment, the presence of 2−3 nm or more PDMAEMA reduced the θ_w of the BC brush to that of a PDMAEMA homopolymer brush. After hexane treatment, the PBMA dominated the surface in the response region, where the PDMAEMA block was relatively short. In the partial-response region, PBMA and PDMAEMA coexisted at the air interface. Further increase of h_{PD} suppressed the rearrangement that allowed the PBMA segments to occupy the air interface after solvent treatment. In the non-response region, a thick PDMAEMA block suppressed the rearrangement of the PBMA and occupied the surface. With gradient substrates of different uniform bottom PBMA block length, we also investigated how the bottom block length affected the solvent response behavior of the BC brushes. θ_w results suggest that increasing the bottom PBMA brush thickness improved the response behavior of the polymer brushes. This change is explained by the PBMA segment's abilities to stretch from the surface and cover the collapsed domains of PDMAEMA.

This work was facilitated by the use of a variety of combinatorial samples, which allowed observation of phenomena that would otherwise be difficult to discern with uniform samples. The gradients were used to (1) characterize the kinetics of surface-initiated ATRP of BMA and DMAEMA, (2) probe the influence of PBMA block length on the ATRP initiating efficiency of DMAEMA, and (3) determine the effect of the relative block length on the BC brushes' response to solvent.

Acknowledgment. C.X. was supported by the Israel−US binational and NSF (CHE-013559) grants to C.M.D. The authors thank Dr. Thomas H. Epps III for helpful discussions. This work was carried out in the NIST Combinatorial Methods Center (NCMC). More information can be found at www.nist.gov/combi.

Supporting Information Available: AFM images of gradient II after hexane treatment. This material is available free of charge via the Internet at http://pubs.acs.org.

References and Notes

(1) Halperin, A.; Tirrell, M.; Lodge, T. P. *Adv. Polym. Sci.* **1991**, *100*, 31−71.

(2) Sanchez, I. C. *Physics of Polymer Surfaces and Interfaces*; Butterworth: London, 1992.
(3) Grest, G. S. *Adv. Polym. Sci.* **1999**, *138*, 149−183.
(4) Zhao, B.; Brittain, W. J. *Prog. Polym. Sci.* **2000**, *25*, 677−710.
(5) Edmondson, S.; Osborne, V. L.; Huck, W. T. S. *Chem. Soc. Rev.* **2004**, *33*, 14−22.
(6) Luzinov, I.; Minko, S.; Tsukruk, V. V. *Prog. Polym. Sci.*. **2004**, *29*, 635−698.
(7) Sidorenko, A.; Minko, S.; Schenk-Meuser, K.; Duschner, H.; Stamm, M. *Langmuir* **1999**, *15*, 8349−8355.
(8) Draper, J.; Luzinov, I.; Minko, S.; Tokarev, I.; Stamm, M. *Langmuir* **2004**, *20*, 4064−4075.
(9) Kim, J.-B.; Huang, W.; Bruening, M. L.; Baker, G. L. *Macromolecules* **2002**, *35*, 5410−5416.
(10) Zhao, B.; Brittain, W. J.; Zhou, W.; Cheng, S. Z. D. *J. Am. Chem. Soc.* **2000**, *122*, 2407−2408.
(11) Boyes, S. G.; Brittain, W. J.; Weng, X.; Cheng, S. Z. D. *Macromolecules* **2002**, *35*, 4960−4967.
(12) Huang, W.; Kim, J.-B.; Baker, G. L.; Bruening, M. L. *Nanotechnology* **2003**, *14*, 1075−1080.
(13) Kong, X.; Kawai, T.; Abe, J.; Tyoda, T. *Macromolecules* **2001**, *34*, 1837−1844.
(14) Zhao, B.; He, T. *Macromolecules* **2003**, *36*, 8599−8602.
(15) Wu, T.; Efimenko, K.; Genzer, J. *J. Am. Chem. Soc.* **2002**, *124*, 9394−9395.
(16) Wu, T.; Efimenko, K.; Vlcek, P.; Subr, V.; Genzer, J. *Macromolecules* **2003**, *36*, 2448−2453.
(17) Lai, P.; Halperin, A. *Macromolecules* **1992**, *25*, 6693−6695.
(18) Roters, A.; Schimmel, M.; Ruhe, J.; Johannsmann, D. *Langmuir* **1998**, *14*, 3999−4004.
(19) Liu, G.; Zhang, G. *J. Phys. Chem. B* **2005**, *109*, 743−747.
(20) Yim, H.; Kent, M. S.; Huber, D. L.; Satija, S.; Majewski, J.; Smith, G. S. *Macromolecules* **2003**, *36*, 5244−5251.
(21) Tu, H.; Heitzman, C. E.; Braun, P. V. *Langmuir* **2004**, *20*, 8313−8320.
(22) Kaholek, M.; Lee, W.-K.; LaMattina, B.; Caster, K. C.; Zauscher, S. *Nano Lett.* **2004**, *4*, 373−376.
(23) Zhu, X.; DeGraaf, J.; Winnik, F. M.; Leckband, D. *Langmuir* **2004**, *20*, 1459−1465.
(24) Currie, E. P. K.; Sieval, A. B.; Fleer, G. J.; Cohen Stuart, M. A. *Langmuir* **2000**, *16*, 8324−8333.
(25) Ionov, L.; Houbenov, N.; Sidorenko, A.; Stamm, M.; Luzinov, I.; Minko, S. *Langmuir* **2004**, *20*, 9916−9919.
(26) Zhao, B. *Langmuir* **2004**, *20*, 11748−11755.
(27) Tomlinson, M. R.; Genzer, J. *Macromolecules* **2003**, *36*, 3449−3451.
(28) Xu, C.; Barnes, S. E.; Wu, T.; Fischer, D. A.; DeLongchamp, D. M.; Batteas, J. D.; Beers, K. L. *Adv. Mater.*, in press.
(29) Xu, C.; Wu, T.; Drain, C. M.; Batteas, J. D.; Beers, K. L. *Macromolecules* **2005**, *38*, 6−8.
(30) Tomlinson, M. R.; Genzer, J. *Chem. Commun.* **2003**, *12*, 1350−1351.
(31) Xu, C.; Wu, T.; Batteas, J. D.; Drain, C. M.; Beers, K. L.; Fasolka, M. J. *Appl. Surf. Sci.* **2006**, *252*, 2529−2534.
(32) Matyjaszewski, K.; Xia, J. *Chem. Rev.* **2001**, *101*, 2921−2990.
(33) Matyjaszewski, K.; Miller, P. J.; Shukla, N.; Immaraporn, B.; Gelman, A.; Luokala, B. B.; Siclovan, T. M.; Kickelbick, G.; Vallant, T.; Hoffmann, H.; Pakula, T. *Macromolecules* **1999**, *32*, 8716−8724.
(34) Huang, X.; Wirth, M. J. *Macromolecules* **1999**, *32*, 1694−1696.
(35) Prucker, O.; Ruhe, J. *Macromolecules* **1998**, *31*, 592−601.
(36) Jordan, R.; Ulman, A. *J. Am. Chem. Soc.* **1998**, *120*, 243−247.
(37) Jordan, R.; Ulman, A.; Kang, J. F.; Rafailovich, M. H.; Sokolov, J. *J. Am. Chem. Soc.* **1999**, *121*, 1016−1022.
(38) Juang, A.; Scherman, O. A.; Grubbs, R. H.; Lewis, N. S. *Langmuir* **2001**, *17*, 1321−1323.
(39) Husseman, M.; Malmstrom, E. E.; McNamara, M.; Mate, M.; Mecerreyes, D.; Benoit, D. G.; Hedrick, J. L.; Mansky, P.; Huang, E.; Russell, T. P.; Hawker, C. J. *Macromolecules* **1999**, *32*, 1424−1431.
(40) Xu, C.; Wu, T.; Mei, Y.; Drain, C. M.; Batteas, J. D.; Beers, K. L. *Langmuir* **2005**, *21*, 11136−11140.
(41) Equipment, instruments, and materials are identified in the paper to adequately specify the experimental details. Such identification does not imply recommendation by NIST, nor does it imply the materials are necessarily the best available for the purpose.
(42) Lee, S. B.; Russell, A. J.; Matyjaszewski, K. *Biomacromolecules* **2003**, *4*, 1386−1393.
(43) Cassie, A. B.; Baxter, S. *Trans. Faraday Soc.* **1944**, *40*, 546−551.
(44) Wenzel, R. N. *Ind. Eng. Chem. Res.* **1989**, *28*, 988−994.

MA051405C